

## Interferometric differentiation between resonant coherent anti-Stokes Raman scattering and nonresonant four-wave-mixing processes

Daniel L. Marks, Claudio Vinegoni, Jeremy S. Bredfeldt, and Stephen A. Boppart<sup>a)</sup>  
*Beckman Institute for Advanced Science and Technology, Department of Electrical and Computer Engineering, University of Illinois at Urbana-Champaign, 405 N. Mathews, Urbana, Illinois 61801*

(Received 22 June 2004; accepted 4 October 2004)

A major impediment to the use of coherent anti-Stokes Raman scattering (CARS) to identify biological molecules is that the illumination levels required to produce a measurable signal often also produce significant nonresonant background from the medium, especially from water. We present a method of nonlinear interferometry to differentiate between which components of the anti-Stokes signal are resonant and nonresonant. The technique takes advantage of the persistence of intermediate states involved in the resonant process. This method is applicable to most existing pulsed CARS illumination methods and provides for identification of resonant CARS. We demonstrate the method by examining the signals produced by acetone, which exhibits resonance, and water, which does not. © 2004 American Institute of Physics. [DOI: 10.1063/1.1829162]

The combination of microscopy and coherent anti-Stokes Raman scattering (CARS) processes<sup>1-4</sup> is a promising tool to study the composition of biological tissues at micrometer scales. Like two-photon microscopy, CARS microscopy relies on a nonlinear interaction to produce a localized point response in the medium. Unlike two-photon microscopy, CARS utilizes endogenous molecular resonances in the tissue and does not require the introduction of exogenous dyes or markers. Frequently the anti-Stokes signal is small because the desired target molecule is present at a low concentration, and is obscured by a large nonresonant nonspecific four-wave-mixing signal at the same frequency. We utilize interferometry with a nonresonantly generated reference pulse to distinguish the resonant CARS from the nonresonant background. By using the interferometric time gate to reject the early emitted nonresonant signal we identify the desired component of the signal. This is a simplification of the nonlinear interferometric vibrational imaging (NIVI)<sup>5,6</sup> method proposed earlier and is more suited to integration with existing CARS pump/Stokes pulse generation methods.

To see how nonresonant signals and resonant CARS can be separated, consider that nonresonant signals arise from four-wave-mixing processes that are mediated purely by virtual states that exist only as long as the atom is “dressed” by the electromagnetic field. Resonant CARS is produced because a molecular vibrational or rotational state is excited by stimulated Raman scattering (SRS). This persistent excitation can be detected by SRS upconversion even after the exciting radiation ends. In contrast, the nonresonant anti-Stokes signal will fall to zero almost immediately upon removal of either the pump or Stokes fields. Thus anti-Stokes radiation caused by resonant CARS continues to be emitted later than the nonresonant signal. This is the method of time-resolved CARS, but typically the resonant and nonresonant components arrive virtually simultaneously relative to the slow speed of conventional photodetectors, so they must be distinguished in other ways. By using interferometry, the ar-

rival time of the resonant and nonresonant components can be clearly and directly observed.

Our approach is to prepare narrowband pump and Stokes pulses, but with the pump pulse stretched out in time to be at least three times longer than the Stokes pulse. The shorter Stokes pulse coincides with the leading edge of the pump pulse. A simulation of this is shown in Fig. 1. When the overlapping pulses arrive, the molecule is excited by SRS. At the same time, a nonresonant four-wave-mixing signal is emitted. After the Stokes pulse passes, so does the nonresonant signal. However, the molecule remains excited. As the pump continues, the excitation is converted to anti-Stokes radiation by SRS. This produces a resonant anti-Stokes signal similar to that shown in Fig. 1, which has a “tail” unlike the nonresonant anti-Stokes, which coincides with the Stokes pulse alone. By delaying a reference pulse at the anti-Stokes frequency until after the nonresonant signal has passed, the reference acts as an interference gate to reject nonresonant components. We note that instead of being stretched, the pump pulse can be split into a separate earlier pump and later probe pulse to achieve larger temporal separations.

Interferometric time gating is commonly used to characterize the shape of ultrafast pulses.<sup>7,8</sup> These methods typically work by interfering a reference pulse with a known

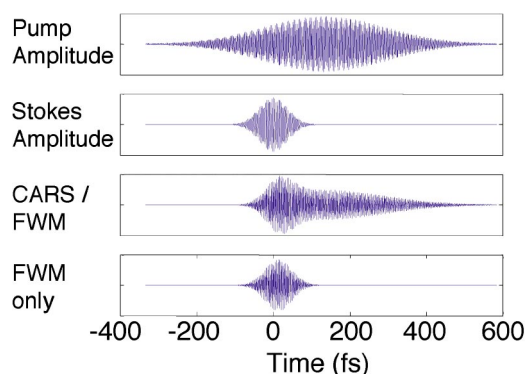


FIG. 1. A simulation of the pulse combination used to differentiate between resonant and nonresonant signals. The pump/Stokes combination overlap to excite CARS, and the anti-Stokes would appear similar to the shown wave form for resonant or nonresonant media.

<sup>a)</sup>Also at: the Department of Bioengineering, the College of Engineering, and the College of Medicine, University of Illinois at Urbana-Champaign, Urbana, IL 61801; electronic mail: boppart@uiuc.edu

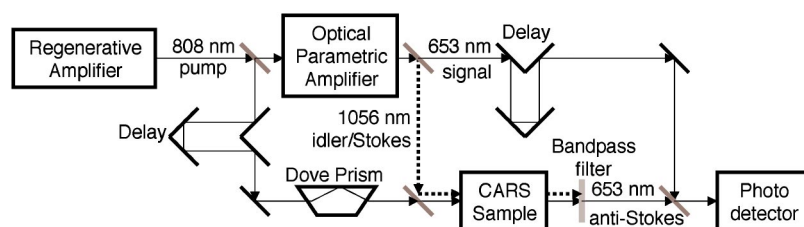


FIG. 2. Schematic of optical setup used to measure the interferogram of resonant and nonresonant signals.

electric field amplitude with an unknown pulse to be characterized. If the reference pulse is short in time compared to the unknown pulse, then interference between the two pulses only occurs over the interval of the reference pulse. By controlling the delay of the two pulses relative to each other, the cross correlation of the two pulses is measured. To obtain the needed short reference pulse, nonresonant four-wave mixing or other cascaded nonresonant nonlinear processes stimulated by short pulses can be used. In particular, a reference pulse delayed until after the nonresonant signal arrives at the photodetector prevents an interference signal from being obtained from the nonresonant component.

The present approach has been motivated by the disadvantages of other approaches of time-resolved CARS for biological imaging. While heterodyning itself adds additional complications, it should be noted that it is a linear interference process, and therefore does not require additional nonlinear process steps that may decrease the overall throughput of the signal generation and collection process. The typical means by which the later time of arrival of the resonant CARS component is distinguished is by observing the anti-Stokes produced by a separate probe pulse which has a polarization,<sup>9</sup> frequency,<sup>10</sup> or illumination angle<sup>11,12</sup> different than the pump and Stokes pulses. Highly scattering tissue is likely to scatter between the polarization states and angular directions, which decrease the nonresonant rejection. Three color methods<sup>13,14</sup> use a probe of a different frequency from the pump to produce a unique anti-Stokes frequency for the resonant CARS signal. These methods can achieve high rejection ratios, but require a new frequency to be generated that is not the pump, Stokes, or anti-Stokes frequencies. While the method we outline must also generate a third frequency, this frequency is identical to the anti-Stokes wavelength, so it can be generated easily with the nonresonant four-wave-mixing process previously mentioned (e.g., in a bulk material such as quartz or water) using just the pump and Stokes.

In addition, heterodyning can offer other advantages. With sufficient reference power, shot noise can exceed thermal noise and stray light noise and therefore photon counting detectors may be unnecessary. Also, by utilizing dual-balanced detection or spectral interferometry, excess noise can be rejected and the interference component can be obtained even with a noisy local oscillator. In microscopy, tight focusing confines the anti-Stokes radiation to a single spatial mode so that it can be overlapped efficiently with the reference pulse. Also, by utilizing a separately generated reference pulse rather than relying on the nonresonant signal of the sample to act as a reference,<sup>15,16</sup> pulse shaping is not required to vary the relative phase between the nonresonant and resonant components, because the delay of the reference pulse can be changed arbitrarily relative to anti-Stokes signal. In addition, a separate reference produces a larger and more constant reference power that is not sample density

dependent, allowing for more quantitative anti-Stokes measurements. This method can potentially be used in conjunction with other methods such as epi-detection<sup>17</sup> and pulse shaping<sup>18</sup> to further minimize the nonresonant component.

To demonstrate and validate this idea, we designed the experiment shown in Fig. 2 to measure the interferograms of anti-Stokes light produced by acetone and water. Acetone has a Raman resonance at  $2925\text{ cm}^{-1}$  corresponding to the C–H stretch, while water does not, containing only hydrogen and oxygen. Water is of primary interest because it is a ubiquitous and pernicious source of nonresonant signal in biological tissues. In the setup, a regenerative amplifier (RegA 9000, Coherent, Inc. Santa Clara, CA) emits pulses at 250 kHz repetition rate with 808 nm center wavelength and 20 nm bandwidth. These pulses are used both as the pump and also to seed a second-harmonic-generation optical parametric amplifier (OPA) (OPA 9450, Coherent) which generates idler pulses with 1056 nm center wavelength and 20 nm bandwidth for use as a Stokes pulse. A 105 mm length BK7 glass Dove prism disperses the pump pulse to approximately three times the duration of the Stokes pulse. Note that there is a difference between the purpose of chirping the pulses here, and that of chirped CARS (c-CARS).<sup>19</sup> Chirping in this technique is done only to lengthen the pump pulse slightly so it only partially overlaps with the Stokes, while in c-CARS it stretches the pulse to be essentially monochromatic over the lifetime of the resonance. The pump pulse is delayed to arrive at a dichroic beamsplitter at the same time as the Stokes pulse. The pulses, which are overlapped and focused into the sample by a 30 mm focal length lens, produce anti-Stokes radiation centered at 653 nm. The OPA signal is produced by two cascaded nonresonant three-wave-mixing steps that produce the same frequency as the four-wave-mixing process but with a far greater amount of power. Because the signal pulse is converted by nonresonant nonlinearities, and the OPA output is adjusted to maximize power, it is reasonable to expect the signal and idler are nearly transform-limited, and therefore will act as a brief time gate. The pump power at the sample was 20 mW, while the Stokes was 2 mW, with sufficient peak power to produce abundant resonant and nonresonant signals. At the same time, the signal pulse from the OPA, also at 653 nm, is used as the reference pulse. A Mach-Zehnder interferometer is used to combine the reference pulse and the CARS signal. The signals are attenuated by neutral density filters by many orders of magnitude before they are detected by a photomultiplier tube. By scanning the relative delay between the two signals, their interferometric cross correlation was measured.

Figure 3 shows the interferograms measured from acetone. The upper left inset shows the Raman spectrum of acetone near the probed resonance frequency. As can clearly be seen, the interferograms agree qualitatively with Fig. 1. The acetone, having a persistent resonance, generates a resonant anti-Stokes “tail” with a length limited not by the life-

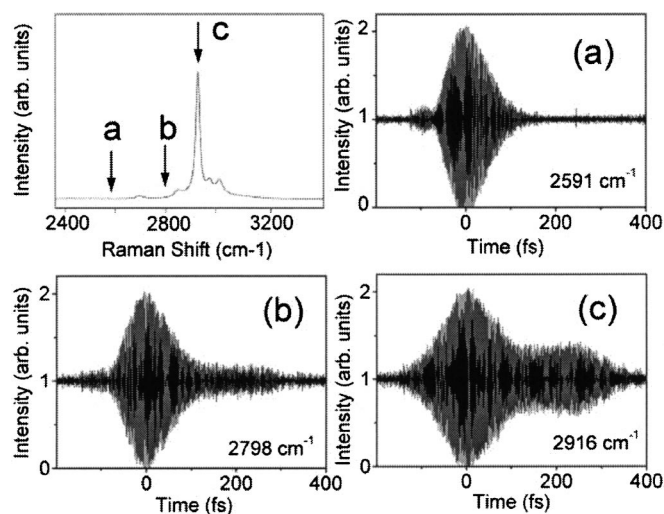


FIG. 3. Partial Raman spectrum of acetone (upper left), and the cross-correlation interferogram of four-wave mixing in acetone at various vibrational excitation frequencies (a)–(c).

time of the resonance but by the length of the pump pulse, because the pump is needed to produce anti-Stokes radiation. As the pump/Stokes frequency difference is tuned away from the resonance at  $2925\text{ cm}^{-1}$ , the resonant “tail” disappears. The tuning resolution is limited by the broad Stokes bandwidth of approximately  $150\text{ cm}^{-1}$ , which is much wider than the Raman susceptibility linewidth, so that the slight inaccuracy of tuning the pump/Stokes difference to  $2916\text{ cm}^{-1}$  instead of  $2925\text{ cm}^{-1}$  had very little effect on the generated resonant signal. To further test the ability to distinguish resonant and nonresonant materials, we filled a cuvette with acetone and water in various volumetric ratios. The concentration of acetone was inferred by observing the amount of power (total magnitude squared signal) in the resonant tail more than 120 fs after the nonresonant peak. Figure 4 shows the interferogram measured from water alone in the inset, which has no tail and is purely nonresonant. As the percent-

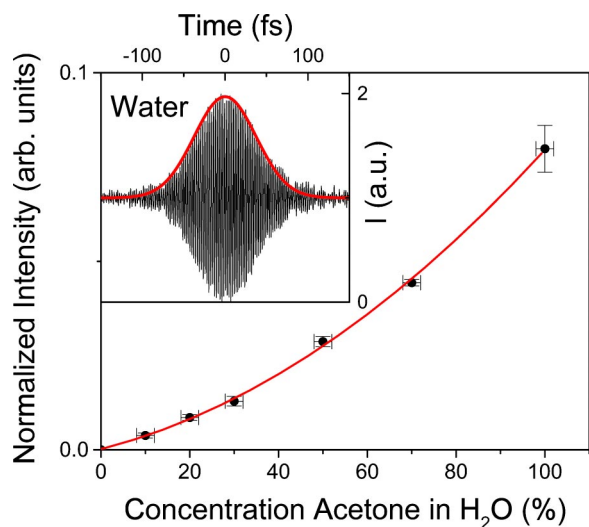


FIG. 4. Interferogram of nonresonant four-wave mixing in water (inset), and the power of the resonant anti-Stokes signal for various percentages of acetone in water by volume.

age of acetone is increased the power of the anti-Stokes signal interference increases quadratically, exactly as expected, as shown in Fig. 4. This demonstrates that the local oscillator remains stable enough to produce an accurate concentration measurement, whereas a nonresonant signal derived from the sample itself may fluctuate with material density and composition.

We have demonstrated a difference in the temporal evolution of anti-Stokes pulses produced by nonresonant and resonant four-wave-mixing processes. While in this proof-of-principle experiment the power utilized was large and the delay mechanism was too slow for practical scanning, we expect the acquisition rate of this detection method can be significantly increased by utilizing a rapidly dithered delay, or single-shot cross-correlation methods.<sup>7,8</sup> This approach utilizes nonlinear interferometry and appropriate reference and excitation pulses to measure the tail of resonant CARS. Such an approach will likely be very useful in CARS microscopy and NIVI<sup>5,6</sup> to eliminate the nonresonant background signal, in addition to the other advantages that interferometric detection can provide such as heterodyne sensitivity and stray light rejection.

The helpful comments of P. Scott Carney are greatly appreciated. The authors also acknowledge the scientific contributions and advice from Martin Gruebele, Dana Dlott, Amy Wiedemann, and Barbara Kitchell from the University of Illinois at Urbana-Champaign. This research was supported in part by the National Aeronautics and Space Administration (NAS2-02057), the National Institutes of Health (National Cancer Institute), and the Beckman Institute for Advanced Science and Technology.

<sup>1</sup>E. O. Potma, D. J. Jones, J.-X. Cheng, X. S. Xie, and J. Ye, *Opt. Lett.* **27**, 1168 (2002).

<sup>2</sup>J.-X. Cheng, Y. K. Jia, G. Zheng, and X. S. Xie, *Biophys. J.* **83**, 502 (2002).

<sup>3</sup>N. Dudovich, D. Oron, and Y. Silberberg, *Nature (London)* **418**, 512 (2002).

<sup>4</sup>M. D. Duncan, J. Reintjes, and T. J. Manuccia, *Opt. Lett.* **7**, 350 (1982).

<sup>5</sup>D. L. Marks and S. A. Boppart, *Phys. Rev. Lett.* **92**, 123905 (2004).

<sup>6</sup>C. Vinegoni, J. S. Bredfeldt, D. L. Marks, and S. A. Boppart, *Opt. Express* **12**, 331 (2004).

<sup>7</sup>K. G. Purchase, D. J. Brady, and K. Wagner, *Opt. Lett.* **18**, 2129 (1993).

<sup>8</sup>L. Lepetit, G. Cheriaux, and M. Joffre, *J. Opt. Soc. Am. B* **12**, 2467 (1995).

<sup>9</sup>J.-X. Cheng, L. D. Book, and X. S. Xie, *Opt. Lett.* **26**, 1341 (2001).

<sup>10</sup>A. Volkmer, L. D. Book, and X. S. Xie, *Appl. Phys. Lett.* **80**, 1505 (2002).

<sup>11</sup>E. Gershgoren, R. A. Bartels, J. T. Fourkas, R. Tobey, M. M. Murnane, and H. C. Kapteyn, *Opt. Lett.* **28**, 361 (2003).

<sup>12</sup>R. Leonhardt, W. Holzappel, W. Zinth, and W. Kaiser, *Chem. Phys. Lett.* **133**, 373 (1987).

<sup>13</sup>F. M. Kamga and M. G. Sceats, *Opt. Lett.* **5**, 126 (1980).

<sup>14</sup>J. J. Song, G. L. Easley, and M. D. Levenson, *Appl. Phys. Lett.* **29**, 967 (1976).

<sup>15</sup>D. Oron, N. Dudovich, and Y. Silberberg, *Phys. Rev. Lett.* **89**, 273001 (2002).

<sup>16</sup>G. W. H. Wurpel, J. M. Schins, and M. Muller, *J. Phys. Chem. B* **108**, 3400 (2004).

<sup>17</sup>A. Volkmer, J.-X. Cheng, and X. S. Xie, *Phys. Rev. Lett.* **87**, 023901 (2001).

<sup>18</sup>D. Oron, N. Dudovich, and Y. Silberberg, *Phys. Rev. Lett.* **90**, 213902 (2002).

<sup>19</sup>K. P. Knutsen, J. C. Johnson, A. E. Miller, P. B. Petersen, and R. J. Saykally, *Chem. Phys. Lett.* **387**, 436 (2004).